Available online at www.sciencedirect.com

SciVerse ScienceDirect

Procedia Engineering 00 (2017) 000–000

Procedia Engineering

www.elsevier.com/locate/procedia

26th International Meshing Roundtable, IMR26, 18-21 September 2017, Barcelona, Spain

Projections for Resolving Delaunay Encroachment

Mark Eastlick[a,*], Carlos Bedregal[b]

[a] *Silvaco Europe Ltd., Compass Point, St. Ives, Cambridge, PE27 5JL, UK*
[b] *Silvaco, Inc., 4701 Patrick Henry Drive, Santa Clara, CA 95054, USA*

Abstract

An efficient method for sampling the features of piecewise smooth domains in the context of restricted Delaunay triangulation is presented. This scheme is based on off-center refinement and is designed to minimize the number of samples needed to correctly resolve the topology of the input. Nearest-point projection is used in regions away from features intersecting at acute angles and circular projection avoids the explicit protection machinery used by other methods where such sharp features occur. We provide a comparison with two standard approaches demonstrating the significant reduction of vertices in the final triangulation.

Peer-review under responsibility of the scientific committee of the 26th International Meshing Roundtable.

Keywords: Restricted Delaunay Triangulation, Encroachment, Circular Projection, Nearest-point Projection, Local Feature Size

1. Introduction

A fundamental area of Technology Computer-Aided Design (TCAD) is concerned with the numerical simulation of physics of semiconductor devices designed electronically. Typically, these devices are represented by a triangulation which must have certain properties if an effective simulation can be performed. At a basic level, the geometry of the device must be adequately captured but the vertex sampling must also be optimized to balance the trade-off between accuracy and resources needed by the computation.

Restricted Delaunay triangulation is a promising method for simultaneously producing surface and volume triangulations of complex domains [1]. Conventionally, such methods produce a vertex sampling proportional to the so-called *local feature size* (lfs) [2]. In addition, sharp features in the input domain may need special treatment, potentially leading to a fixed sampling of these areas [3, 4]. This can translate into unnecessarily dense, inflexible meshes for TCAD applications leading to computationally expensive simulations.

In this paper we introduce two complimentary dimension-independent approaches for sampling the input domain in the context of restricted Delaunay triangulation. The first, *nearest-point projection*, is used away from sharp features and avoids the lfs-based sampling of standard methods. The second, *circular projection*, is applied around sharp areas and ensures termination of the sampling process. Compared to other strategies, these methods do not require weighted Delaunay triangulation, knowledge of the lfs, or preprocessing to explicitly protect sharp features [1].

* Corresponding author. Tel.: +44-1480-424400 ; fax: +44-1480-424401.
E-mail address: mark.eastlick@silvaco.com

Peer-review under responsibility of the scientific committee of the 26th International Meshing Roundtable.

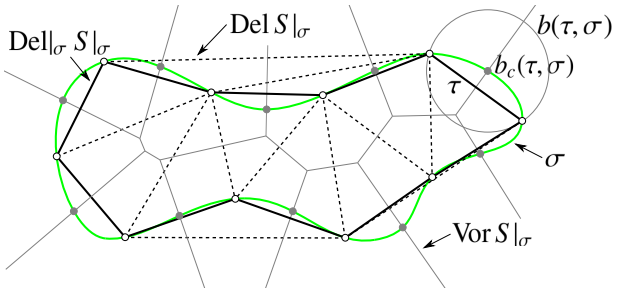

Fig. 1: Restricted Delaunay sub-complex $\mathrm{Del}|_\sigma S|_\sigma$ for 1-cell σ as subset of Delaunay triangulation $\mathrm{Del}\, S|_\sigma$ and relationship to Voronoi diagram $\mathrm{Vor}\, S|_\sigma$, including Delaunay ball $b(\tau, \sigma)$ for 1-simplex $\tau \in \mathrm{Del}|_\sigma S|_\sigma$.

2. Resolving Encroachment via Projections

A fundamental part of methods based on Delaunay refinement is the resolution of encroachment. This ensures that features of the input domain are resolved by the simplices in the final triangulation by constructing a sampling which contains sets of vertices which have circumscribing spheres which are empty of other vertices. The *de facto* method for resolving encroachment inserts the center of such spheres, leading to a sampling proportional to the local feature size which may be undesirably dense. In this section we describe two *off-center* refinement rules with the object to minimize the number of vertices needed to resolve the topology of the input domain.

2.1. Preliminaries

This subsection contains basic definitions used throughout the document. For brevity, we omit the standard definitions of a cell σ and piecewise smooth complex (PSC) $\mathcal{S}$ [1]. A piecewise linear complex (PLC) is viewed as a special-case of a PSC where the cells are flat. Figure 1 shows a 2-dimensional example of constructs in this section.

Definition 2.1. Let $\mathcal{S} \subset \mathbb{R}^n$ be a PSC, $S = \{p : p \in \mathcal{S}\}$ be a set of point samples and $\sigma \in \mathcal{S}_l$ be an l-cell for $0 \leq l < n$. The restriction of S to σ is $S|_\sigma = S \cap \sigma$.

Definition 2.2. Let $\sigma \in \mathcal{S}_l$ be an l-cell, $\tau \in \mathrm{Del}\, S|_\sigma$ be a Delaunay l-simplex and $\tau^* \in \mathrm{Vor}\, S|_\sigma$ be its dual Voronoi $(n-l)$-cell. The simplex τ is called *restricted* if $\tau^* \cap \sigma \neq \varnothing$. The Delaunay sub-complex $\mathrm{Del}|_\sigma S|_\sigma$ is the union of the restricted l-simplices:

$$\mathrm{Del}|_\sigma S|_\sigma = \bigcup_{\tau^* \cap \sigma \neq \varnothing} \tau. \tag{1}$$

Definition 2.3. Let $\sigma \in \mathcal{S}_l$ be an l-cell, $\tau \in \mathrm{Del}|_\sigma S|_\sigma$ be a restricted Delaunay l-simplex and $\tau^* \in \mathrm{Vor}\, S|_\sigma$ be its dual Voronoi cell. A circumscribing sphere of τ is a called a *Delaunay ball* $b(\tau, \sigma)$ if its center $b_c(\tau, \sigma)$ and radius $b_r(\tau, \sigma)$ satisfy

$$b_c(\tau, \sigma) \in \tau^* \cap \sigma, \quad b_r(\tau, \sigma) = |p_\tau - b_c(\tau, \sigma)|, \tag{2}$$

where p_τ is a 0-simplex of τ.

Definition 2.4. Let $\tau \in \mathrm{Del}|_\sigma S|_\sigma$ be a restricted Delaunay l-simplex and $p \in \mathbb{R}^n$ be a point. The simplex τ is *encroached* by p if $|p - b_c(\tau, \sigma)| < b_r(\tau, \sigma)$.

Remark. If the Delaunay ball of simplex $\tau \in \mathrm{Del}|_\sigma S|_\sigma$ is not encroached by any $p \in S$ then $\tau \in \mathrm{Del}\, S$, provided that $\mathrm{Del}\, S$ is unique.

Definition 2.5. Let $\tau \in \mathrm{Del}|_\sigma S|_\sigma$, $\upsilon \in \mathrm{Del}|_\varrho S|_\varrho$ be restricted Delaunay simplices. These are called *siblings* if $\tau \cap \upsilon \neq \varnothing$.

Remark. If the largest principal angle between the pair of subspaces in which the siblings lie is smaller than $\pi/2$ then *ping pong encroachment* can occur if refinement using centers of the Delaunay balls is used (Figure 2a). This may lead to non-termination of Delaunay refinement.

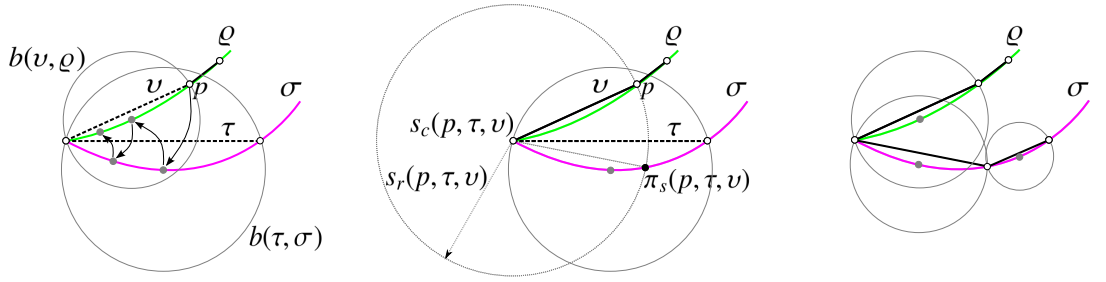

(a) (b) (c)

Fig. 2: (a) Mutual encroachment of 1-simplices τ and υ caused by a sharp feature of 1-cells σ and ϱ. (b) Encroached restricted 1-simplex τ and sphere of projection $s(p, \tau, \upsilon)$. (c) Result of refinement by circular projection $\pi_s(p, \tau, \upsilon)$.

2.2. Refinement by Nearest Point Projection

If a restricted l-simplex τ is encroached by a point p which does not belong to one of its siblings then we perform *nearest point projection* of this point onto the l-cell σ corresponding to τ and this point is added to the triangulations instead. This encroaching point may already be in S but it can also arise as a candidate to insert in the triangulation which is then superseded by its projection.

Definition 2.6. Let $p \in \mathbb{R}^n$ be a point and $\sigma \in \mathcal{S}_l$ be an l-cell. The *nearest point projection* $\pi_n : \mathbb{R}^n \to \sigma$ satisfies

$$\pi_n(p) = \underset{q \in \sigma}{\arg\min} \, |q - p| \,. \tag{3}$$

Refinement by nearest point projection is equivalent to orthogonal projection of the encroaching point p onto the l-cell to which the encroached simplex belongs.

2.3. Refinement by Circular Projection

If a restricted l-simplex τ is encroached by a vertex of one of its sibling simplices then we perform *circular projection* of this point onto the l-cell σ corresponding to τ and this point is added to the triangulations instead.

Definition 2.7. Let $\tau \in \mathrm{Del}|_\sigma \, S|_\sigma$, $\upsilon \in \mathrm{Del}|_\varrho \, S|_\varrho$ be restricted Delaunay siblings and $p \in \mathbb{R}^n$ be a point. The *sphere of projection* $s(p, \tau, \upsilon)$ has center $s_c(p, \tau, \upsilon)$ and radius $s_r(p, \tau, \upsilon)$ which satisfy

$$s_c(p, \tau, \upsilon) = \underset{q \in \tau \cap \upsilon}{\arg\min} \, |q - p| \,, \quad s_r(p, \tau, \upsilon) = |p - s_c(p, \tau, \upsilon)| \,. \tag{4}$$

The intersection $\tau \cap \upsilon$ is a single point if the dimension of either sibling simplex is one. This covers all possibilities for $\mathcal{S} \subset \mathbb{R}^2$ and all but one of those for $\mathcal{S} \subset \mathbb{R}^3$. The final situation is when the intersection corresponds an edge shared between a pair of 2-simplices. In this case, $s_c(p, \tau, \upsilon)$ can be calculated via the orthogonal projection of p onto the subspace of this edge.

Definition 2.8. Let $\tau \in \mathrm{Del}|_\sigma \, S|_\sigma$, $\upsilon \in \mathrm{Del}|_\varrho \, S|_\varrho$ be restricted Delaunay siblings and $s(p, \tau, \upsilon)$ be the sphere of projection. The *circular projection* $\pi_s : s(p, \tau, \upsilon) \to \sigma$ satisfies

$$\pi_s(p, \tau, \upsilon) = \underset{q \in s(p, \tau, \upsilon) \cap \sigma}{\arg\min} \, |q - p| \,. \tag{5}$$

For $\mathcal{S} \subset \mathbb{R}^3$, the point p and circular projection point $\pi_s(p, \tau, \upsilon)$ lie on a great circle of the sphere of projection. For the case of projection onto a 2-cell $\sigma \in \mathcal{S}_2$, the tangent vector of this great circle coincides with the normal vector of σ at $\pi_s(p, \tau, \upsilon)$. The projection point for a 1-cell $\sigma \in \mathcal{S}_1$ is an intersection of σ with $s(p, \tau, \upsilon)$, see Figure 2c.

Remark. In their basic form, the projections of Definitions 2.6 and 2.8 may produce a sampling of the input domain whose vertices are arbitrarily close together. In practice, we reject a candidate refinement point if it lies within ϵ distance of a vertex of the encroached simplex τ and use the center of its Delaunay ball $b_c(\tau, \sigma)$ instead.

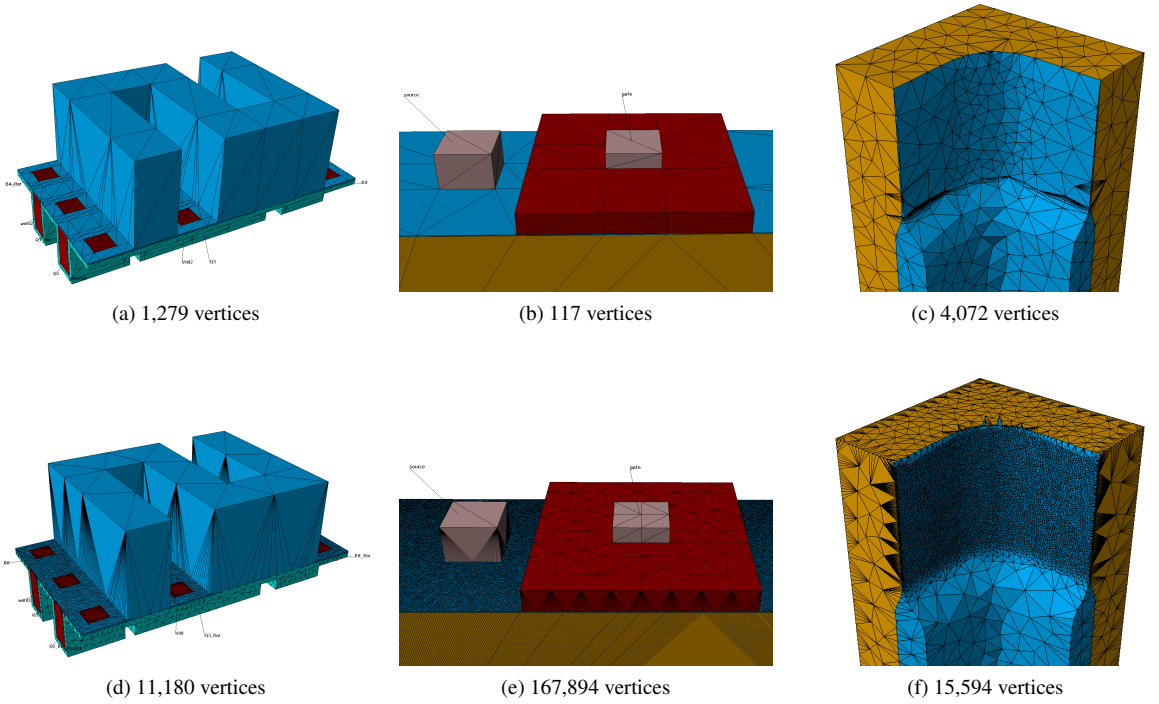

(a) 1,279 vertices (b) 117 vertices (c) 4,072 vertices

(d) 11,180 vertices (e) 167,894 vertices (f) 15,594 vertices

Fig. 3: Comparison of number of vertices for `radex08`, `powerex18` and `powerex20` devices. (a), (b), (c) `UNIFIED-off_center`. (d), (e) `UNIFIED-circumcenter`. (f) `CGAL-Mesh3`.

3. Empirical Evaluation

We evaluated the performance of the restricted Delaunay algorithm based on the definitions in Section 2, referred to as `UNIFIED` throughout. For PLC inputs, we compare the performance of `UNIFIED` using the projection schemes presented in Sections 2.2 and 2.3, referred to as `UNIFIED-off_center`, with a variation of the algorithm using the traditional resolution of encroachment via centers of Delaunay balls, referred to as `UNIFIED-circumcenter`. The input domains correspond to two different TCAD devices: a six transistor 22nm SRAM cell `radex08` and a buffered super junction LDMOS `powerex18`. For PSC inputs, we compare `UNIFIED-off_center` with an implementation of `CGAL-Mesh3` (version 4.7) [5] customized to ensure that the protecting balls do not intersect disjoint patches. For this test we use a vertical LOCOS power MOSFET device `powerex20`. Note that `UNIFIED-circumcenter` cannot be used in this context because it does not guarantee termination in the context of sharp features in the input domain.

The first and second columns in Figure 3 show the triangulations generated by `UNIFIED-off_center` (top) and `UNIFIED-circumcenter` (bottom). These *minimal* triangulations represent the first instance in the sampling procedure where there topology of the input is correctly represented. The excessive sampling of the thin layers produced by the circumcenter-based approach is proportional to the lfs of the layer. Using the off-center approach, we can effectively minimize the number of vertices needed to represent the topology, greatly reducing the number of vertices of the initial triangulation for the refinement stage. The third column in Figure 3 shows the resulting triangulations after applying uniform refinement to a PSC device generated by `UNIFIED-off_center` (top) and `CGAL-Mesh3` (bottom). Again, the thin material is sampled beyond the required element size; a condition imposed by the traditional approach to resolve encroachments. The off-center method is able to represent the same device for the same element size constraints with almost four times fewer vertices.

Figure 4 shows that refined triangulations of PLC and PSC devices using `UNIFIED-off_center` also outperforms traditional approaches. For the PLC case (Figure 4a) as long as the circumradius bound is larger than the lfs of the thin

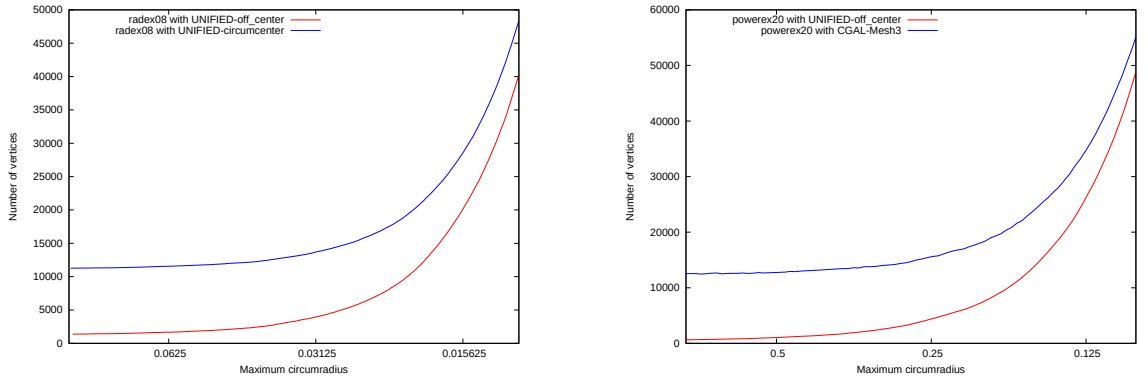

(a) (b)

Fig. 4: Comparison of number of vertices as a function of maximum circumradius. (a) PLC device `radex08`. (b) PSC device `powerex20`.

layer, `UNIFIED-off_center` would produce significantly fewer vertices than `UNIFIED-circumcenter`. Note that the gap in performance is even more extreme with devices including a higher proportion of thin layers. We observe the same behavior with PSC devices (Figure 4b). An additional factor contributing to the reduced number of vertices generated by `UNIFIED-off_center` is the use of circular projections around sharp features (Section 2.3), completely eliminating the need of extra samplings to protect sharp features as used by conventional restricted Delaunay algorithms such as `CGAL-Mesh3`.

4. Conclusions

A unified vertex sampling scheme for restricted Delaunay meshing has been described which is based on projections of encroaching points. These are designed with the aim of minimizing interactions between disjoint vertices and simplices of the triangulation. Sharp features in the input domain are dealt with by a general method based on circular projections which compliments the nearest-point approach in other regions.

It has been shown empirically that the off-center refinement schemes described here combine to significantly reduce the number of vertices needed to resolve the topology of TCAD devices when compared with conventional strategies based on insertion of centers of Delaunay balls. A practical benefit is that a greater proportion of vertices can be used to optimize the triangulation to ensure efficient and reliable simulation of the physics of the device.

References

[1] S.-W. Cheng, T. K. Dey, J. Shewchuk, Delaunay Mesh Generation, 1st ed., Chapman & Hall/CRC, 2012.
[2] J. Ruppert, A delaunay refinement algorithm for quality 2-dimensional mesh generation, J. Algorithms 18 (1995) 548–585.
[3] T. K. D. Siu-wing Cheng, J. A. Levine, A practical delaunay meshing algorithm for a large class of domains, in: Proceedings of the 16th International Meshing Roundtable, 2007, pp. 477–494.
[4] D. Engwirda, Conforming restricted delaunay mesh generation for piecewise smooth complexes, Procedia Engineering 163 (2016) 84 – 96. 25th International Meshing Roundtable.
[5] C. Jamin, S. Pion, M. Teillaud, 3D triangulations, CGAL User and Reference Manual, 4.7 ed. (2015).